Ageing-induced structural evolution of mechanically alloyed $Ga_{40}Se_{60}$

2008 J. Phys.: Condens. Matter 20 345226

(http://iopscience.iop.org/0953-8984/20/34/345226)

J. Phys.: Condens. Matter **20** (2008) 345226 (3pp) doi:10.1088/0953-8984/20/34/345226

Ageing-induced structural evolution of mechanically alloyed $Ga_{40}Se_{60}$

S M de Souza[1], J C de Lima[2], C E M Campos[2], T A Grandi[2] and D M Trichês[1]

[1] Departamento de Engenharia Mecânica, Universidade Federal de Santa Catarina, Campus Universitário Trindade, S/N, CP 476, 88040-900 Florianópolis, Santa Catarina, Brazil
[2] Departamento de Física, Universidade Federal de Santa Catarina, Campus Universitário Trindade, S/N, CP 476, 88040-900 Florianópolis, Santa Catarina, Brazil

Received 22 April 2008, in final form 29 June 2008
Published 6 August 2008
Online at stacks.iop.org/JPhysCM/20/345226

Abstract
After four years of ageing at room temperature, a nanocrystalline $Ga_{40}Se_{60}$ alloy produced by mechanical alloying was re-investigated using x-ray diffraction and differential scanning calorimetry techniques. The results show that this sample, mainly a monoclinic Ga_2Se_3 phase, evolved to a multi-phase crystalline alloy, mainly a trigonal Se one, containing also minority crystalline phases. The monoclinic Ga_2Se_3 phase remains visible after ageing and the nucleation of the Se–O and Se phases is attributed to migration of Se atoms located at interfacial components of the as-milled sample. Similar ageing effects were also observed for a portion of $Ga_{40}Se_{60}$ alloy annealed four years ago.

1. Introduction

Nanocrystalline materials are composed of two components: one crystalline, equal to that found in the bulk materials, and another, called interfacial, which is formed by centers of defects, such as grain boundaries, interphases, and dislocations. The numbers of atoms present in the two components are similar. It is well known that defect centers accumulate energy. With defect elimination through any process, the released stored energy may promote structural evolution and nucleation of new phases. The literature shows several papers reporting the evolution and nucleation of new phases with ageing. De Lima *et al* reported that the atomic structure of amorphous selenium (a-Se) produced by MA [1], which is formed with an ordinary Se_n chain-like shape, transformed partially to an Se_8 ring-like shape with ageing at ambient temperature and pressure. In another paper [2], those workers reported results for the ageing of a ZnSe alloy produced by MA at ambient conditions. They found that the ageing promoted the growth of c-Se clusters/agglomerates, and attributed this fact to the probable presence of small quantity of c-Se seeds in the interfacial component of the as-milled ZnSe sample. More recently, an amorphous GaSe alloy produced by MA by the same group of workers [3] presented a partial amorphous–crystalline transformation with ageing at ambient conditions. The main crystalline phase was the trigonal Se, but high-pressure Se phases were also proposed [4].

In the present paper, we propose to verify ageing effects on as-milled and annealed nanocrystalline $Ga_{40}Se_{60}$ alloys produced by MA in 2004 (named *aged*-$Ga_{40}Se_{60}$ and *aged–annealed*-$Ga_{40}Se_{60}$, respectively). For this, x-ray diffraction (XRD) and differential scanning calorimetry (DSC) are used.

2. Experimental procedure

Four years prior to measurements, a nanocrystalline $Ga_{40}Se_{60}$ sample was produced by MA using high-purity elemental gallium ingots and selenium powder. Its XRD pattern showed the monoclinic Ga_2Se_3 phase and a minority amorphous phase. Part of the *as-milled*-$Ga_{40}Se_{60}$ sample was annealed at 450 °C (*annealed*-$Ga_{40}Se_{60}$) and only the monoclinic Ga_2Se_3 phase remained. Further details can be found in [5]. Both *as-milled*-$Ga_{40}Se_{60}$ and *annealed*-$Ga_{40}Se_{60}$ samples were kept at ambient conditions.

The XRD measurements were performed using a Philips X-Pert powder diffractometer, equipped with graphite monochromator, and using Cu Kα radiation ($\lambda = 1.5418$ Å). Rietveld analyses of the XRD patterns were carried out using the DBWS 9708 code and pseudo-Voigt functions defining peak profiles.

The DSC measurements were performed using a TA 2010 equipment operating from 25 to 500 °C with a heating rate of 10 °C min^{-1}, under flowing nitrogen.

Table 1. Lattice parameters of the *aged*-$Ga_{40}Se_{60}$ and *aged–annealed*-$Ga_{40}Se_{60}$ samples.

	ICSD* JCPDS**			As-milled and aged samples			Annealed and aged samples		
Phase	*a* (Å)	*b* (Å)	*c* (Å)	*a* (Å)	*b* (Å)	*c* (Å)	*a* (Å)	*b* (Å)	*c* (Å)
Ga_2Se_3	6.661*	11.652*	6.649*	6.650	11.633	6.618	6.644	11.632	6.623
c-Se	4.366**	4.366**	4.954**	4.363	4.363	4.937	4.355	4.355	4.945
Se(ortho)	4.006*	6.017*	2.628*	3.970	6.036	2.631	3.997	6.026	2.625
SeO_2	8.322**	8.322**	5.054*	8.349	8.349	5.057	8.295	8.295	5.044

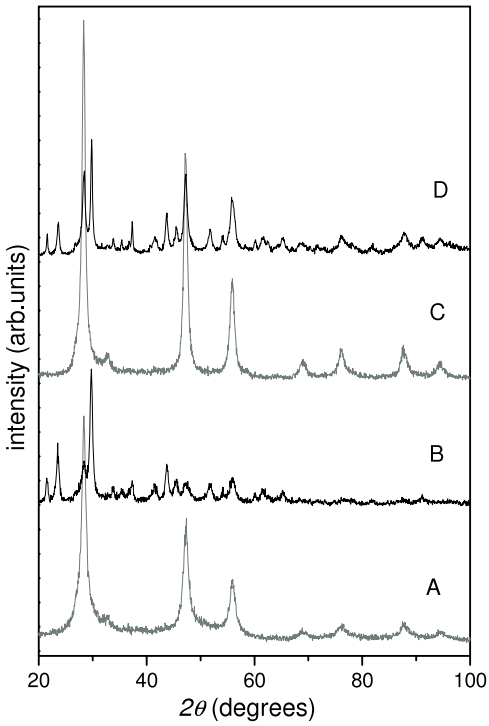

Figure 1. XRD patterns for the *as-milled*-$Ga_{40}Se_{60}$ (A), *aged*-$Ga_{40}Se_{60}$ (B), *annealed*-$Ga_{40}Se_{60}$ (C) and *aged–annealed*-$Ga_{40}Se_{60}$ (D) samples.

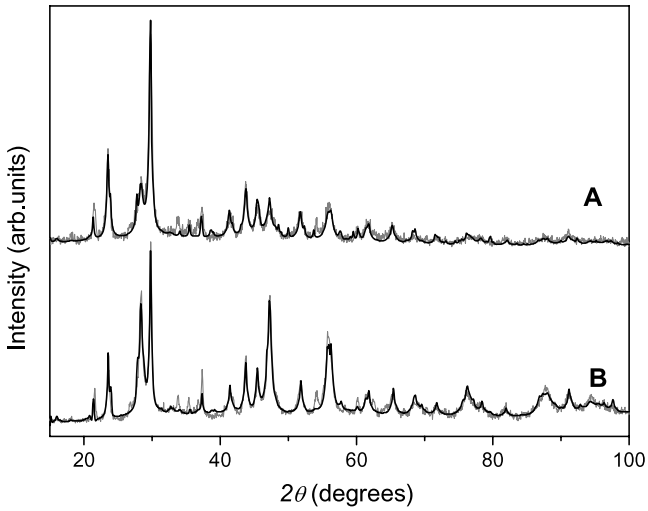

Figure 2. Experimental (gray lines) and calculated (black lines) XRD patterns of the *aged*-$Ga_{40}Se_{60}$ (A) and *aged–annealed*-$Ga_{40}Se_{60}$ (B) samples.

3. Results and discussion

3.1. XRD measurements

Figure 1 shows the XRD pattern of the *as-milled*-$Ga_{40}Se_{60}$ (curve A) and *aged*-$Ga_{40}Se_{60}$ (curve B) samples. In this figure are also shown the patterns for the *annealed*-$Ga_{40}Se_{60}$ (curve C) and *aged–annealed*-$Ga_{40}Se_{60}$ (curve D) samples. The Rietveld analyses of the A and C curves were already reported in [5]. In the B and D curves the peaks belonging to the monoclinic Ga_2Se_3 phase had their intensities decreased due to ageing. These patterns also show reflections associated with trigonal Se (ICSD [6] card no 22251), SeO_2 (ICSD card no 72367), SeO_3 (ICSD card no 18180) and orthorhombic selenium (JCPDS [7] card no 471516). The reappearance of trigonal Se with ageing at ambient conditions was already observed in [1, 2] and [4]. It is interesting to note that the orthorhombic phase is a high-pressure Se one reported for pressures higher than 28 GPa [8] and one possible explanation for this is that MA is a method based on the action of high non-hydrostatic pressure, which could be responsible for the formation of very small seeds of this high-pressure phase. In the following it will be shown that its inclusion improves considerably the Rietveld fittings (see peaks at $2\theta = 37.3°$ and 60.0° in figure 2).

In order to quantify the crystalline phase fractions in the *aged*-$Ga_{40}Se_{60}$ and *aged–annealed*-$Ga_{40}Se_{60}$ samples, their XRD patterns were analyzed by using the Rietveld refinement method [9]. The structural model was based on the ICSD cards of trigonal selenium, Ga_2Se_3, SeO_2, SeO_3 and the JCPDS card of orthorhombic selenium, for which the coordinates were taken from an atlas of crystal structures [10]. The best fittings and lattice parameters are shown in figure 2 and table 1, respectively. The lattices parameter changes with ageing are not conclusive. Probably these changes are related to the atomic diffusion processes in the interfacial component and new phase formation. The crystalline phase fractions obtained for the *aged*-$Ga_{40}Se_{60}$ were: trigonal Se (50%), Ga_2Se_3 (24%), SeO_2 (14%) and orthorhombic selenium (11%). For the *aged–annealed*-$Ga_{40}Se_{60}$, they were: trigonal Se (50%), Ga_2Se_3 (46%), SeO_2 (2%) and orthorhombic selenium (8%). We can see that Ga_2Se_3 phase is more stable in the annealed sample than in the as-milled sample. MA processes can create a specific state of the surface, possibly with special surface defects and imperfections that may facilitate the diffusion mechanisms. In this way, the diffusion mechanisms and atomic electronegativity may provide information about the preference of formation of selenium phases. The Se atoms (ratio = 1.22 Å) are 33% smaller than the Ga atoms (ratio = 1.81 Å);

Table 2. Average crystallite size and microstrain of the *as-milled*-$Ga_{40}Se_{60}$, *annealed*-$Ga_{40}Se_{60}$*aged*-$Ga_{40}Se_{60}$ and *aged–annealed*-$Ga_{40}Se_{60}$ samples.

Sample	$\langle d \rangle$ (Å)	σ (%)
As-milled [5]	75	2.0
Annealed [5]	105	1.8
This work		
As-milled and aged	119	0.9
Annealed and aged	420	0.4

this means that the Se atoms migrate faster than Ga atoms. Their atomic electronegativities are 1.6 eV for Ga and 2.4 eV for selenium which is close to that for oxygen (3.5 eV). Therefore we believe that selenium phases nucleated first and the Ga atoms are diluted in the interfacial component, without crystalline structure.

The average crystallite size $\langle d \rangle$ and microstrain σ_p were also obtained from the Rietveld analysis through the relationship

$$\left(\frac{\beta_t \cos\theta}{K\lambda}\right)^2 = \frac{1}{\langle d \rangle^2} + \sigma_p^2 \left(\frac{\sin\theta}{K\lambda}\right)^2,$$

where θ is the diffraction angle, λ is the x-ray wavelength, β_t is the total broadening measured at the peak's full width at half-maximum (FWHM) in radians, and K is the Scherrer constant (=0, 91). The values obtained are listed in table 2. One can see that considerable crystallite growth and microstrain reduction occurred due to ageing.

3.2. DSC measurements

Figure 3 shows the DSC curves for the *as-milled*-$Ga_{40}Se_{60}$ (curve A), *aged*-$Ga_{40}Se_{60}$ (curve B) and *aged–annealed*-$Ga_{40}Se_{60}$ (curve C) samples. The curve A, already presented in [5], shows only an exothermic feature associated with the crystallization of the amorphous fraction observed for the *as-milled*-$Ga_{40}Se_{60}$. The curves B and C are quite similar and show three endothermic features. The first one, between 100 and 170 °C, is associated with water release, that located at 217 °C corresponds to melting of trigonal selenium and the third one (350–440 °C) could be correlated with melting of SeO_2 and SeO_3 oxides (316 and 394 °C, respectively [11]) but the presence of SeO_3 oxide is not supported by XRD. Up to now we have no unambiguous explanation for the third endothermic feature.

4. Conclusions

Two nanometric $Ga_{40}Se_{60}$ samples (one as-milled and another annealed) produced by MA four years prior to measurements were aged at ambient conditions. These samples were re-investigated using XRD and DSC techniques and important ageing effects were observed. The main observations are the following.

(1) DSC measurements on both as-milled and aged, and annealed and aged samples showed melting points associated with the trigonal selenium and selenium oxides, evidencing that the ageing of the samples promoted the nucleation and growth of these phases.

(2) Simulations of the XRD patterns measured for the as-milled and aged, and annealed and aged samples using the Rietveld refinement method showed that part of the nanometric monoclinic Ga_2Se_3 phase present in the as-milled and annealed samples together with the atomic configurations present in their interfacial components transformed with ageing trigonal selenium and selenium oxides.

(3) The balance of the monoclinic Ga_2Se_3 phase remains in the nanometric form and it is more stable in the annealed sample than in the as-milled sample.

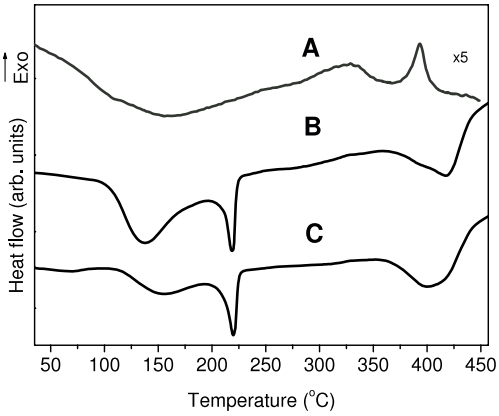

Figure 3. DSC curves: *as-milled*-$Ga_{40}Se_{60}$ (A), *aged*-$Ga_{40}Se_{60}$ (B) and *aged–annealed*-$Ga_{40}Se_{60}$ (C) samples.

Acknowledgments

We thank the CAPES, CNPq and FAPESC agencies for financial support. We are indebted to Dr Patricia Bodanese for the XRD measurements.

References

[1] de Lima J C, Grandi T A and de Biasi R S 2001 *J. Non-Cryst. Solids* **93** 286
[2] Machado K D, de Lima J C, Campos C E M and Gasperini A A M 2003 *Solid State Commun.* **127** 477
[3] Campos C E M, de Lima J C, Grandi T A, Machado K D and Pizani P S 2003 *Solid State Commun.* **126** 611
[4] Campos C E M, de Lima J C, Grandi T A, Souza S M and Pizani P S 2007 *Solid State Commun.* **142** 270
[5] Souza S M, Campos C E M, de Lima J C, Grandi T A and Pizani P S 2006 *Solid State Commun.* **139** 70
[6] 1995 *Inorganic Crystal Structure Database (ICSD)* Gmelin-Institut für Anorganische Chemie and Fachinformationszentrum, FIZ Karlsruhe
[7] *JCPDS: Joint Committee on Powder Diffraction Standards (Philadelphia)* 2000
[8] Akahama Y, Kobayashi M and Kawamura H 1992 *Solid State Commun.* **83** 269
[9] Rietveld H M 1969 *J. Appl. Crystallogr.* **2** 65
[10] Daams L C, Villars P and Van Vucht J H N 1991 *Atlas of Crystal Structure Types For Intermetallic Phases* (Materials Park, OH: ASM International) p 2507
[11] de Lima J C, Schmitt M, Grandi T A, Campos C E M, Höln H, Souza S M and Trichês D M 2007 *J. Phys.: Condens. Matter* **19** 186216